Food Hydrocolloids 69 (2017) 440–449

Contents lists available at ScienceDirect

Food Hydrocolloids

journal homepage: www.elsevier.com/locate/foodhyd

Development of eggless cakes suitable for lacto-vegetarians using isolated pea proteins

Muyang Lin [a, b], Siang Hong Tay [a], Hongshun Yang, Ph.D. [a, b, *], Bao Yang [c], Hongliang Li [d]

[a] Food Science and Technology Programme, c/o Department of Chemistry, National University of Singapore, Singapore, 117543, Singapore
[b] National University of Singapore (Suzhou) Research Institute, 377 Lin Quan Street, Suzhou Industrial Park, Suzhou, Jiangsu 215123, PR China
[c] Key Laboratory of Plant Resources Conservation and Sustainable Utilization, Guangdong Provincial Key Laboratory of Applied Botany, South China Botanical Garden, Chinese Academy of Sciences, Guangzhou, Guangdong 510650, PR China
[d] Guangzhou Welbon Biological Technology Co., Ltd., 232 Kezhu Rd., Guangzhou, Guangdong 510663, PR China

ARTICLE INFO

Article history:
Received 26 November 2016
Received in revised form
10 February 2017
Accepted 8 March 2017

Keywords:
Cake
Pea protein
Xanthan gum
Emulsifier
Fourier transform infrared spectroscopy (FTIR)
Atomic force microscopy (AFM)

ABSTRACT

Cakes are important confectionery and are enjoyed socially within groups. Eggs are important components of cakes, providing emulsification, flavour, colour, and many other properties. However, because of various health concerns and religious beliefs, some consumers cannot enjoy traditional cakes made with eggs. In the current study, isolated pea protein (PPI), xanthan gum (XN), and emulsifier mixtures were investigated to prepare eggless cakes and their roles were determined. The physicochemical properties of the batter and final cake products, the microstructure of the final cakes, and structural properties of starches and glutens at the meso-scale were characterised. The eggless cake recipe containing PPI, 0.1% XN and 1% soy lecithin (SL) was found to be close to the control traditional cakes in terms of specific gravity (1.01 *vs.* 1.03), crumb colour (a^* at 0.09 *vs.* −0.04), and crumb pore properties (average pore area both 0.20 mm^2). Cakes with formulation R4 were most similar to the control cakes with respect to the 1047/1022 relative intensity of the IR spectra of starches (both 0.55) and the nanostructures of glutenins. Therefore, formulation PPI+0.1% XN+ 1% SL was considered as a potential candidate recipe for substituting eggs in cakes.

1. Introduction

Cakes are one of the most widely consumed and enjoyed cereal products, with an ever-increasing global market demand. One of the most important ingredients in cakes is eggs. Eggs have an important function in the foam formation of the batter, as air is incorporated into the batter during the mixing stage and gel setting as the liquid foam (batter) turns into a solid foam (cake) during baking. The unique gel setting property of eggs is essential to provide cakes with their volume, specific texture qualities, colours, and flavours (Kiosseoglou & Paraskevopoulou, 2014). However, besides the prevalence of egg allergy in the paediatric population, the growing trend in lacto-vegetarians, increased rate of heart diseases, high price of eggs, and limited cold chain distribution for certain countries/areas, have increased the demand for eggless cakes.

As a result, many studies have evaluated proteins as potential candidates for egg substitutes, from various sources including soy (Rahmati & Mazaheri Tehrani, 2014), pea (Hoang, 2012) and whey proteins (Ratnayake, Geera, & Rybak, 2012). Currently, however, few have developed an eggless cake that matches cakes made with eggs in terms of their physical properties. This suggested that many egg substitutes are multicomponent, and it would be advisable to consider the application of proteins together with hydrocolloids and emulsifiers to develop egg substitutes. Furthermore, the use of plant proteins and emulsifiers might provide additional nutrients and improve nutrient delivery to the consumers (Mao & Miao, 2015).

Image analysis of the macrostructures of baked products is a relatively simple and quick method to detect the visual differences among crumbs (Turabi, Sumnu, & Sahin, 2010). Currently, no studies have used image analysis of the substitutes of eggs in cakes. Thus, in the present study, image analysis was performed to determine the differences in pore attributes between cakes made with different formulations. In addition, the structures of the major components at

* Corresponding author. Food Science and Technology Programme, c/o Department of Chemistry, National University of Singapore, Singapore, 117543, Singapore.
E-mail address: chmynghs@nus.edu.sg (H. Yang).

http://dx.doi.org/10.1016/j.foodhyd.2017.03.014
0268-005X/

the molecular level were also investigated for eggless cakes. Fourier transform infrared (FTIR) spectroscopy and atomic force microscopy (AFM) are used widely to study the structural changes of macromolecules in food samples because of their ease of use. FTIR spectroscopy can provide information on molecular interactions, such as bonding, ordering, and secondary structure. (Luo, Lui, Xu, Ionescu, & Petrovic, 2013; Sow & Yang, 2015; Wang, Su, Schulmerich, & Padua, 2013). By contrast, AFM provides more direct visualisation of a molecule's conformation and is suited to characterising macromolecules, including pectin, gelatin, and starch, (An et al., 2011; Chong, Lai, & Yang, 2015; Du, An, Liu, Yang, & Wei, 2014; Feng, Bansal, & Yang, 2016; Feng, Fu, & Yang, 2017; Liu, Tan, Yang, & Wang, 2017; Yang, 2014; Zhang, Chen, Zhang, Lai, & Yang, 2017). Therefore, AFM and FTIR spectroscopy were adopted to access the conformations of the starches and glutens.

The aim of this project was to develop egg substitutes for cakes using pea proteins and plant polysaccharide mixture. The effects of hydrocolloids and emulsifiers on the batter properties and physical properties of eggless cakes were evaluated. Finally, structural analysis at the meso-scale was conducted to better understand the mechanism of action of the effects of the additions to the cake ingredients.

2. Material and methods

2.1. Ingredients

The yellow cake recipe by (Ratnayake et al., 2012), with slight modifications, was used in this study. Table 1 lists the recipes of the control cakes and the eggless cakes with different substitutes, denoted by R1 – R4. Flour was provided by PRIMA RND (Prima Group, Singapore); the rest of the ingredients (sugar, fresh eggs, baking powder, canola oil, and skimmed milk) were obtained from a local supermarket (Fairprice, Singapore). The egg substitute ingredients used were xanthan gum (XN) (Grindstead®) and soy lecithin (SL) (SOLEC®), obtained from Danisco (S) Pte Ltd (Singapore, Singapore); mono and diglycerides (MDG) (Emulpals 110®) from Palsgaard Asia Pacific Pte Ltd (Singapore, Singapore); corn starch from Ingredion Singapore Pte Ltd (Singapore, Singapore); and isolated pea protein (PPI) (80% w.b.) from Shaanxi Fuheng Biotechnology Co. Ltd (Shaanxi, China).

2.2. Preparation of cake batter and baking

The dry ingredients (cake flour and baking powder) were sifted and added into the mixer (KitchenAid, St Joseph, MI, USA) containing the wet ingredients (sugar, milk, eggs and canola oil). The ingredients were first homogenised for 1 min at speed 1 and subsequently mixed at speed 6 for 4 min. Two hundred and 50 g of batter were measured into baking tins and baked in a convection oven (Fabricant Eurfours®, Gommegnies, France) pre-heated at 180 °C for 35 min. The cakes were kept at room temperature to cool for 60 min before performing the analyses.

Table 1
Formulations of control cakes and eggless cakes with different substitutes.

Ingredients	Composition (%)				
	Control	R1	R2	R3	R4
Cake flour	27.88	27.88	27.88	27.88	27.88
Milk	16.73	16.73	16.73	16.73	16.73
Eggs	13.93	–	–	–	–
Baking powder	0.84	0.84	0.84	0.84	0.84
Canola oil	8.36	8.36	8.36	8.36	8.36
Sugar	32.26	32.26	32.26	32.26	32.26
PPI	–	3.48	3.48	3.48	3.48
XN	–	–	0.1	0.1	0.1
MDG	–	–	–	1	–
SL	–	–	–	–	1
Corn starch	–	1.11	1.01	0.01	0.01
Water	–	9.34	9.34	9.34	9.34

*R1: PPI; R2: PPI + 0.1% XN; R3: PPI + 0.1% XN + 1% MDG; R4: PPI + 0.1% XN + 1% SL. PPI – isolated pea protein; XN – xanthan gum; MDG – mono, diglycerides and SL – soy lecithin.

2.3. Physicochemical properties of eggless cakes

2.3.1. Characterisation of the batter

The specific gravity of the batter was measured by filling a cylindrical cup with batter. The mass of the batter was taken relative to the mass of water using the same cup. The specific gravity was calculated using the formula:

$$\text{Specific gravity} = \text{mass of batter/mass of water at } 25\ ^\circ\text{C}$$

A Rapid Viscosity Analyser series 4 (Newport Scientific Pty Ltd., Jessup, MD, USA) was used to measure the batter viscosity, according to Wilderjans, Pareyt, Goesaert, Brijs, and Delcour (2008). The programme Thermocline for windows version 2.4 (Newport Scientific Pty Co., Ltd.) was used to set the parameters for analysis. For the analysis, the temperature profile was based on the internal temperature of the batter during baking. The paddle speed was set at 75 rpm.

2.3.2. Characterisation of the cakes

The volume of the finished product was measured using the Stable Microsystem Volscan profiler 600 (Stable Micro Systems Ltd., Surrey, UK). The specific volume of the cake was determined with the volume and the mass of the final cake using the following formula:

$$\textit{Specific Volume} = \frac{\textit{Volume}}{\textit{Mass}}$$

The textural properties of the cakes were measured according to Ratnayake et al. (2012), with some modifications. Cake samples were cut into cubes (20 mm × 20 mm × 20 mm) and the textural properties were determined using a TA-XT2i texture analyser (Stable Micro System Ltd., Surrey, UK) with a 25 mm cylinder probe. A double compression test was performed. For compression testing, the parameters were set accordingly: pre-test speed = 5 mm/s, test speed = 1 mm/s, and post-test speed = 1 mm/s. The compression distance = 10 mm. Firmness and springiness were calculated according to the previous reported methods (Mao et al., 2017; Yang, Wu, Ng, & Wang, 2017).

The moisture content of the samples was measured according to AOAC procedures (Horwitz, 1980), in which 2.0 ± 0.1 g of cake crumbs were dried in an oven (100 °C) for at least 24 h and the weight difference was recorded before and after drying. The colour parameters (CIE L*, a* and b* values) of the cake crumb were measured using a Kinoca Minolta CM-5 spectrophotometer (Konica Minolta Holdings, Inc., Tokyo, Japan). Plastic cling wrap was used as a reference. The overall colour difference, which is denoted by ΔE, was determined using the following formula:

$$\Delta E = \sqrt{\left(L^* - L^*_{ref}\right)^2 + \left(a^* - a^*_{ref}\right)^2 + \left(b^* - b^*_{ref}\right)^2}.$$

2.3.3. Image analysis of cakes

A method similar to that of Hicsasmaz, Yazgan, Bozoglu, and

Katnas (2003) was used. A 1 cm thick cross-section of the cakes was used. The cakes were painted with a black oil based ink to delineate the pores. A Nikon DS5100 digital camera (Nikon Corporation, Tokyo, Japan) was used to capture the images (3 mm^2 > pore area >0.01 mm^2). To reveal the details (pore area <0.01 mm^2), an Olympus SZ61 (Olympus, Melville, NY) stereomicroscope with a camera attachment and a zoom range of 6.7–40 × was used. Thresholding was performed to obtain a black and white image of the pore wall skeleton using ImageJ2 software (National Institutes of Health, USA). A histogram of the pore area, equivalent to the sum of the calibrated pixel units, was constructed using Microsoft Excel.

2.4. Extractions of starches and glutens

Cake samples were cut into small pieces and freeze-dried after removing the crust parts. The dry crumbs (10 g) were defatted with 100 mL of hexane for 1 h three times (Wilderjans et al., 2008). The samples were then dried under a stream of nitrogen. The starch samples were extracted based on the method described by Xie, Cui, Li, and Tsao (2008). The defatted sample (2 g) was soaked in 10 mL of 70% ethanol for 18 h. After draining the steep liquor, 5 mL of distilled water was added before grinding the sample. The samples were screened with 100-Mesh followed by 200-Mesh sieves, followed by centrifugation at 3000 × *g*. Then, 0.5 M NaOH solution (10 mL) was added with stirring for 20 min, followed by centrifugation. The pellet was extracted with 10 mL of an H_2O/toluene (4:1 v/v) mixture. The supernatant was collected and centrifuged to obtain the starch isolate.

The gluten protein fractions were separated using a modified Osborne approach (Lookhart & Bean, 1995; Wang et al., 2014; Zhang, Lu, Yang, & Meng, 2011). The defatted samples (2 g) were first treated with deionised water (10 mL) and then with 0.5 M NaCl aqueous solution (10 mL) for 30 min each. The suspensions were subject to centrifugation at 7000 × *g* for 5 min, with the rinsed with deionised water. The pellet was then extracted with 70% ethanol (10 mL) for 30 min at 4 °C. The supernatants after the centrifugations contained the gliadins. Subsequently, a mixture solution of dithiothreitol (1%) and n-propanol (50%) (5 mL) was applied to the residue at 4 °C. The glutenin subunits were obtained by centrifuging the suspension after 30 min of extraction.

2.5. Wide angle powder XRD determination

The freeze-dried crumb samples were ground into fine powder and subjected to powder X-ray diffraction (XRD) analysis using a Siemens D5005 diffractometer (Bruker AXS, Karlsruhe, Germany), which was equipped with a copper tube operating at 40 kV and 40 mA. The parameters were set at 7–30° for analysis in the 2θ range, 0.01° for the step size, and 1 s per 2θ interval for the measurement time (Primo-Martín, van Nieuwenhuijzen, Hamer, & van Vliet, 2007). After baseline being subtracted and $K\alpha_2$ peak stripped, the integrated areas were measured using DIFFRAC plus EVA 10.0.1.0 (Bruker AXS, Karlsruhe, Germany). Relative crystallinity was calculated using the following formula (Miao, Jiang, Zhang, Jin, & Mu, 2011):

$$X_C = \frac{A_c}{A_c + A_a},$$

where, X_C was the relative crystallinity, and A_c and A_a were the integrated areas of crystalline and amorphous regions, respectively.

2.6. FTIR analysis of starch and gluten proteins

The dry samples were blended with KBr (1% w/w) to prepare thin discs and the spectra were collected using a Spectrum One FTIR spectrometer (PerkinElmer, Waltham, MA, USA) at 4 cm^{-1} resolution for 32 scans in the range of 4000–450 cm^{-1}. The FTIR spectra were interpreted using the Omnic software 8.2 (Thermo Fisher Scientific Inc., Waltham, MA, USA). For the starch spectra, Fourier self-deconvolution was applied in the range of 1100 to 950 cm^{-1} and the intensity ratios of the peaks at 1047 and 1022 cm^{-1} were recorded from the spectra.

The amide III regions (1350–1200 cm^{-1}) in the spectra of gliadins and glutenins were analysed using the second derivative function. The derivative spectra were obtained from the eleven-point, two-degree polynomial function and then multiplied by −1 to invert the peaks. Finally, the corresponding components and their relative contents were acquired with the OriginPro 9.0 software (OriginLab, Northampton, MA, USA). The glutenin spectra were also studied by deconvolution at the amide I band (1700-1600 cm^{-1}) to provide complementary information. Gaussian peak fitting was conducted on the deconvoluted spectra in the OriginPro 9.0 software, according to Byler and Susi (1986). The relative contents of the secondary structures were obtained from the relative integrated areas of the corresponding fitted peaks.

2.7. Morphology analysis of glutens

The extracted gliadin and glutenin solutions were diluted to 0.1 mg/mL with 70% aqueous ethanol solution and 50% n-propanol, respectively. The diluted solution (10 μL) was then dropped onto a freshly prepared mica sheet and dispersed with the help of a blower (Liu et al., 2017). Upon drying, the morphological analyses of protein fractions were performed using a table top (TT)-AFM (AFM workshop, Signal Hill, CA, USA), which was equipped with an AppNano ACLA-10 probe (Applied NanoStructures, Mountain View, CA, USA) with resonance frequencies of 145–230 kHz and force constants of 36–90 N/m. The qualitative and quantitative analyses of the images were carried out with the AFM offline software, Gwyddion (http://gwyddion.net) (Feng, Ng, Mikš-Krajnik, & Yang, 2017; Sow & Yang, 2015).

2.8. Statistical analysis

Each experiment was conducted in triplicate and the results were presented as the mean ± standard deviation. Statistical analyses using analysis of variance (ANOVA) and Duncan's multiple range test for differences among different cakes were conducted using IBM SPSS Statistics 21.0 (IBM Corp., Chicago, IL, USA). Comparisons that yielded a P value < 0.05 were considered significant.

3. Results and discussion

3.1. Batter properties of eggless cakes baked with different formulations

Batter and cake properties were analysed after preliminary baking using the selected formulations (Table 1). The results of the physical attributes of batters and cakes are shown in Table 2. The viscosity of the eggless cake batters was significantly (P < 0.05) higher than that of the control batter (27.08–36.17 *vs.* 4.05 Pa s). Viscous batter slowed down the rate of gas escape from the batter during baking (Wilderjans et al., 2008), thus preventing shrinkage during baking. Conversely, if the batter was too viscous, it impeded aeration during the mixing step, resulting in a denser batter and a smaller final product. However, xanthan gum had a unique rod like conformation and is more responsive to shear (Ashwini, Jyotsna, & Indrani, 2009), which explained that despite the batter of R2 being viscous, it still aerated better than R1 during mixing giving the

Table 2
Batter, crumb, and starch ordering parameters of eggless cakes using isolated pea protein (PPI) and other baking additives as egg substitutes.

Group	Control	R1	R2	R3	R4
Initial viscosity (Pa s)	4.05 ± 0.12^{D}	34.82 ± 3.43^{A}	36.17 ± 4.46^{A}	31.17 ± 1.71^{B}	27.08 ± 1.97^{C}
Specific gravity	1.03 ± 0.00^{BC}	1.13 ± 0.02^{A}	1.08 ± 0.01^{B}	0.95 ± 0.07^{D}	1.01 ± 0.01^{CD}
Specific volume (cm^3/g)	2.17 ± 0.03^{A}	1.38 ± 0.04^{D}	1.51 ± 0.01^{C}	1.80 ± 0.03^{B}	1.87 ± 0.02^{B}
Firmness (g)	362.3 ± 45.7^{B}	1118.1 ± 125.3^{A}	1050.1 ± 117.5^{A}	344.1 ± 77.4^{B}	237.7 ± 35.7^{C}
Springiness (%)	95.0 ± 3.1^{A}	83.0 ± 5.0^{B}	77.0 ± 2.0^{CD}	73.0 ± 5.0^{DE}	69.0 ± 1.0^{E}
Moisture (%)	29.02 ± 0.48^{A}	27.33 ± 0.37^{C}	28.16 ± 0.89^{B}	28.51 ± 0.98^{AB}	27.02 ± 0.22^{C}
L*	77.88 ± 1.65^{A}	72.68 ± 0.67^{C}	75.12 ± 1.80^{B}	72.81 ± 1.45^{C}	69.02 ± 0.80^{D}
a*	-0.04 ± 0.31^{D}	1.74 ± 0.11^{A}	1.83 ± 0.09^{A}	1.15 ± 0.07^{B}	0.09 ± 0.31^{CD}
b*	24.56 ± 1.72^{AB}	25.38 ± 0.55^{AB}	25.97 ± 0.75^{A}	23.86 ± 0.48^{B}	19.70 ± 0.62^{C}
ΔE	79.39 ± 0.94^{A}	74.07 ± 0.76^{C}	76.56 ± 1.80^{B}	73.63 ± 1.31^{C}	68.66 ± 0.66^{D}
X_c	0.21 ± 0.03^{B}	0.24 ± 0.01^{AB}	0.27 ± 0.01^{A}	0.26 ± 0.00^{AB}	0.27 ± 0.03^{A}
In(1047/1022)	0.55 ± 0.01^{A}	0.54 ± 0.01^{A}	0.54 ± 0.01^{A}	0.56 ± 0.01^{A}	0.55 ± 0.01^{A}

X_c: Relative crystallinity obtained from X-ray diffraction (XRD); In (1047/1022): Intensity ratio of peaks at 1047 and 1022 cm^{-1} in Fourier transform infrared spectroscopy (FTIR) spectra.
*R1: PPI; R2: PPI + 0.1% XN; R3: PPI + 0.1% XN + 1% MDG; R4: PPI + 0.1% XN + 1% SL. PPI – isolated pea protein; XN – xanthan gum; MDG – mono, diglycerides; SL – soy lecithin. Mean values within the same row with different letters indicate significant differences ($P < 0.05$).

former a less dense batter. The batter viscosity of R4 was the lowest amongst the eggless cake batters (Table 2). This was attributed to the fact that the SL used was in a liquid form and thus provided additional fluidity to the batter. In addition, it could be deduced that the aeration capacity of the emulsifiers had a more dominant effect compared with the viscosity of the batter, thus enabling a lighter cake batter. The batter viscosity played an important role in the final volume of the cake, because a viscous batter was able to retain the gas bubbles diffusing out of the batter during baking (Ashwini et al., 2009).

Replacing eggs with PPI alone (R1) resulted in an increase in the specific gravity of the batter from 1.03 for the control cake to 1.13. This clearly indicated that pea proteins lacked the unique and superior foaming capabilities of eggs. This foaming ability is essential to provide aeration to the cake batter for quality cake production. Upon the addition of XN to the eggless cake mixture (R2), a significant ($P < 0.05$) decrease in the specific gravity (1.08) of the batter was observed, indicating that XN could enhance the foaming ability of PPI in the batter system. The improvement in foaming capacity, coupled with the unique structure of XN, made it more responsive to shear, which could possibly explain the improved specific gravity of R2 batter compared with R1, despite having the same viscosity.

From Table 2, R3 and R4 had a lighter cake batter (specific gravities of 0.95 and 1.01) compared with R2. Application of emulsifiers to cake batters has been known to lower the specific gravity, because emulsifiers provide batter with good aeration capacity (Lakshminarayan, Rathinam, & KrishnaRau, 2006). In addition, emulsifiers also help with the incorporation of air into the batter by reducing the surface tension between the liquid and gas phase, thereby lowering the amount of energy needed to create a larger interfacial area (Sahi & Alava, 2003). In the study of hydrocolloids and emulsifiers on rice cakes, Turabi, Sumnu, and Sahin (2008) observed that a mixture of emulsifiers and xanthan gum gave lower specific gravity compared with xanthan gum alone. However, the different types of emulsifiers used in formulations R3 and R4 provided similar batter specific gravities, without a significant difference, indicating that the decrease in batter specific gravity was caused by the addition of emulsifier and independent of the type of emulsifier used.

3.2. Physical properties of eggless cakes baked with different formulations

The physical properties of cake baked with different recipes are also shown in Table 2. The eggless cakes had significantly lower specific volumes compared with that of the control (2.17 cm^3/g) and increased from R1 to R4 (1.38–1.87 cm^3/g), which was in line with the decreasing batter specific gravity. In the relationship between batter and cake, a lower specific volume results from a lack of aeration during expansion and therefore the lack of expansion of the cake batter during baking, which was observed clearly in Table 2. Works by Ashwini et al. (2009); Gómez, Ronda, Caballero, Blanco, and Rosell (2007), and Sahi and Alava (2003) also showed that the specific volume of a cake is dependent on the batter specific gravity and batter viscosity. Similar observations were made for the eggless cake with formulation R4. CO_2 from the leavening agent and water vapour trapped in the air cells can contribute to the expansion of the incorporated air cell during mixing, and thus increased the batter volume during baking (Ashwini et al., 2009).

The texture profiles of the eggless cakes are also presented in Table 2. R1 and R2 resulted in very firm cakes (1118.1 and 1050.1 g) whereas R3 and R4 resulted in soft crumbs (344.1 and 237.7 g), which were closer to the value of the control (362.3 g). It was reported that emulsifiers can form amylose-lipid complexes with amylose in starch, which alter starch gelatinisation properties (Lakshminarayan et al., 2006) and therefore reduce crumb firmness. As a result, it can be postulated that the emulsifiers formed amylose lipid complexes successfully, thereby providing cakes with their softer textures. On the other hand, the eggless cakes lost some springiness compared with the control cakes (69–83% *vs.* 95%). As the protein aggregation in a cake crumb is related to springiness (Wilderjans et al., 2008), it was hypothesised that the different types of protein present in the eggless formulations (pea proteins) and the control (egg proteins) were responsible for the differences. Plus, egg yolk is not pure protein and contains other particles (e.g. LDL and HDL micelles) that aid in the thermal stabilisation of the yolk gel (Kiosseoglou & Paraskevopoulou, 2014). The reduction of the springiness was more significant in R3 and R4, suggesting that the 1% MDG or SL used in this experiment was the dominant stabilising material (Sahi & Alava, 2003).

Similarly, the eggless cakes had lower moisture contents compared with the control cakes (Table 2). The decrease in moisture content was probably due to the poor moisture retention capability of the eggless cake formulations. Also, the crumb colours of the eggless cakes were darker than the traditional cake (lower L* values) (Table 3). However, there was no significant change in the b* value of the eggless cake compared with the control. Thus, similar light scattering components could be present in the pea proteins.

3.3. Pore size and distribution of eggless cakes

Besides the properties of appearance, the pore quality of the

Table 3
Percentage of secondary structures of gliadin and glutenin in eggless cakes with PPI substitutes.

Group	Secondary structure (%)			
	α-helix	β-sheet^	β-turn	Random coil
Gliadin				
Control	12.53 ± 0.74^{B}	67.14 ± 3.81^{A} (–)	2.96 ± 0.75^{D}	17.37 ± 2.32^{A}
R1	15.75 ± 0.11^{A}	69.01 ± 1.21^{A} (–)	15.24 ± 1.32^{C}	0.11 ± 0.20^{D}
R2	15.42 ± 1.20^{A}	48.70 ± 1.16^{C} (–)	25.74 ± 0.31^{A}	10.15 ± 2.02^{AB}
R3	15.39 ± 1.03^{A}	57.62 ± 2.11^{B} (–)	18.71 ± 0.06^{B}	8.27 ± 3.08^{BC}
R4	11.88 ± 2.87^{B}	44.71 ± 1.15^{C} (–)	27.99 ± 2.43^{A}	15.42 ± 1.16^{A}
Glutenin				
Control	37.37 ± 0.91^{B}	57.12 ± 0.75^{A} (20.45^{b})	–	5.51 ± 1.66^{BC}
R1	34.57 ± 4.91^{BC}	57.27 ± 1.32^{A} (29.10^{a})	–	8.16 ± 4.02^{B}
R2	31.70 ± 2.97^{C}	52.52 ± 5.11^{B} (29.51^{a})	–	15.78 ± 7.96^{A}
R3	42.81 ± 1.37^{A}	52.43 ± 1.09^{B} (20.58^{b})	–	4.77 ± 2.30^{BC}
R4	43.74 ± 0.21^{A}	55.69 ± 0.51^{AB} (20.13^{b})	–	0.57 ± 0.35^{C}

^ Values in parentheses are the relative content of intermolecular β-sheet compared with the total secondary structures.
- Not detected.
*R1: PPI; R2: PPI + 0.1% XN; R3: PPI + 0.1% XN + 1% MDG; R4: PPI + 0.1% XN + 1% SL. PPI – isolated pea protein; XN – xanthan gum; MDG – mono, diglycerides and SL – soy lecithin. Mean values with different letters indicate significantly differences ($P < 0.05$).

cake crumb is also an important consideration when developing egg substitutes for cakes (Lin, Tay, Yang, Yang, & Li, 2017). Fig. 1 displays samples of cakes under the optical microscope and the camera. There were crack like pores in the crumb of the control cake, which resulted from the diffusion pathways of the convection currents in the batter (Hicsasmaz et al., 2003). The buoyancy of air bubbles in the batter is inversely proportional to the batter's viscosity (Baixauli, Sanz, Salvador, & Fiszman, 2008); therefore, the control cake almost lost its cell structures. Thus, the crumbs of the eggless cakes lacked these crack-like structures because of their high viscosity (Table 2), which was in line with a previous report (Baixauli et al., 2008).

Pore size and distribution were used to quantify the differences among the eggless cakes (Fig. 2). R1 and R2 showed smaller average pore sizes to the control, whereas cakes baked with formulation R3 had larger pores. Eggless cakes with PPI + 0.1% XN + 1% SL (R4) as the substitute had a similar average pore size to that of the control. Graph of frequency distribution (Fig. 2b) also indicated that eggless cakes using formulation R4 had the most similar pore size distribution as the control egg cakes for all sizes of pores. This similarity might be explained by the presence of lecithin in both the control and R4 cakes compared with the "whippability" effect of MDG on the cake batter. Sahi and Alava (2003) made similar observations when glyceryl monostearate (GMS) was added to sponge cake batters. Thus, the data suggested that formulation R4 is the most promising formulation to develop eggless cakes with similar crumb pore characteristics to traditional cakes.

3.4. Structural properties of starches

Powder XRD determination was adopted to study the ordering of starch molecules and their relative crystallinities; the results are displayed in Table 2. Among all the diffractograms, there is only one broad peak at 2θ angle of about 20° (equivalent to a d spacing of 4.4 Å), referring to the crystalline V-type amylose-lipid complexes (Primo-Martín et al., 2007). The absence of the other patterns (2θ angles of 15°, 17°, 18° and 23°) in comparison with native starch samples was also observed in previous research (Primo-Martín et al., 2007). It was attributed to the gelatinisation process of amylose upon mixing and heating (Hesso et al., 2015). According to the XRD results, the relative crystallinities of all the groups were as low as 20% and the differences were subtle.

FTIR spectroscopy was used to analyse the structural changes of starch at the molecular level (Fig. 3a). Fig. 3b shows the relative intensities of the peaks at 3434, 1743, and 1083 cm^{-1}. Slight increases in the relative intensity at 3434 cm^{-1} in the eggless cakes (R1-R4) were observed in the spectra. The 3434 cm^{-1} peak reflects the amount of inter- and intra-molecular hydroxyl groups in a starch sample (Ji et al., 2015), and the increment of the peak intensity of the anhydroglucose ring C–O stretching vibration (1021, 1083 and 1156 cm^{-1}) could be attributed to enhanced hydrogen bonds between the starch chains (Ji et al., 2015). As a result, the FTIR spectra indicated a significant decrease in the inter-chain hydrogen bonds in starch molecules in the eggless cakes.

In addition, compared with the control group, a new peak at about 1743 cm^{-1} was found in the FTIR spectra of starch from the eggless cakes, except for the one containing 1% SL (R4) (Fig. 3a). This peak was associated with the stretching vibration of the C=O bond in methyl esters and might indicate the formation of new cross-linking structures (Liu et al., 2014). Also, its appearance coincided with a sharp shoulder at about 2855 cm^{-1}, which was characterised as the absorbance frequency for C–H stretching vibration (Ji et al., 2015). The absence of this carbonyl group in the control and R4 groups could be attributed to the presence of lecithin species, either from the egg yolk or from the added soy lecithin. The slightly charged choline group on lecithin species might compete with the hydroxyl group on starch for the carboxylic group from proteins or other components. In short, the inclusion of lecithin in cakes can reduce the degree of crosslinking to some extent.

The peaks at about 1047 and 1022 cm^{-1} were also demonstrated to be the characteristic peaks for monitoring the crystallinity of starch, being assigned to C–O–H bending in ordered and amorphous starches, respectively (Liu et al., 2014). The ratios of the intensities of these two peaks in Table 2 showed that there were no significant differences between the relative crystallinities of starch samples in the different groups. This result was generally consistent with the one obtained using X-ray diffraction, despite the values of the crystallinity from XRD results being lower. It probably reflected the differences in the principles and scopes between the two analytical methods. FTIR is more sensitive to short-scale ordering in the double helices, while only a longer range of crystallinity (i.e., the ordered packing of double helices) can be accepted as a real crystalline region in XRD (Miao et al., 2011; Primo-Martín et al., 2007).

3.5. FTIR determination of glutens

FTIR spectroscopy was employed to assess the secondary

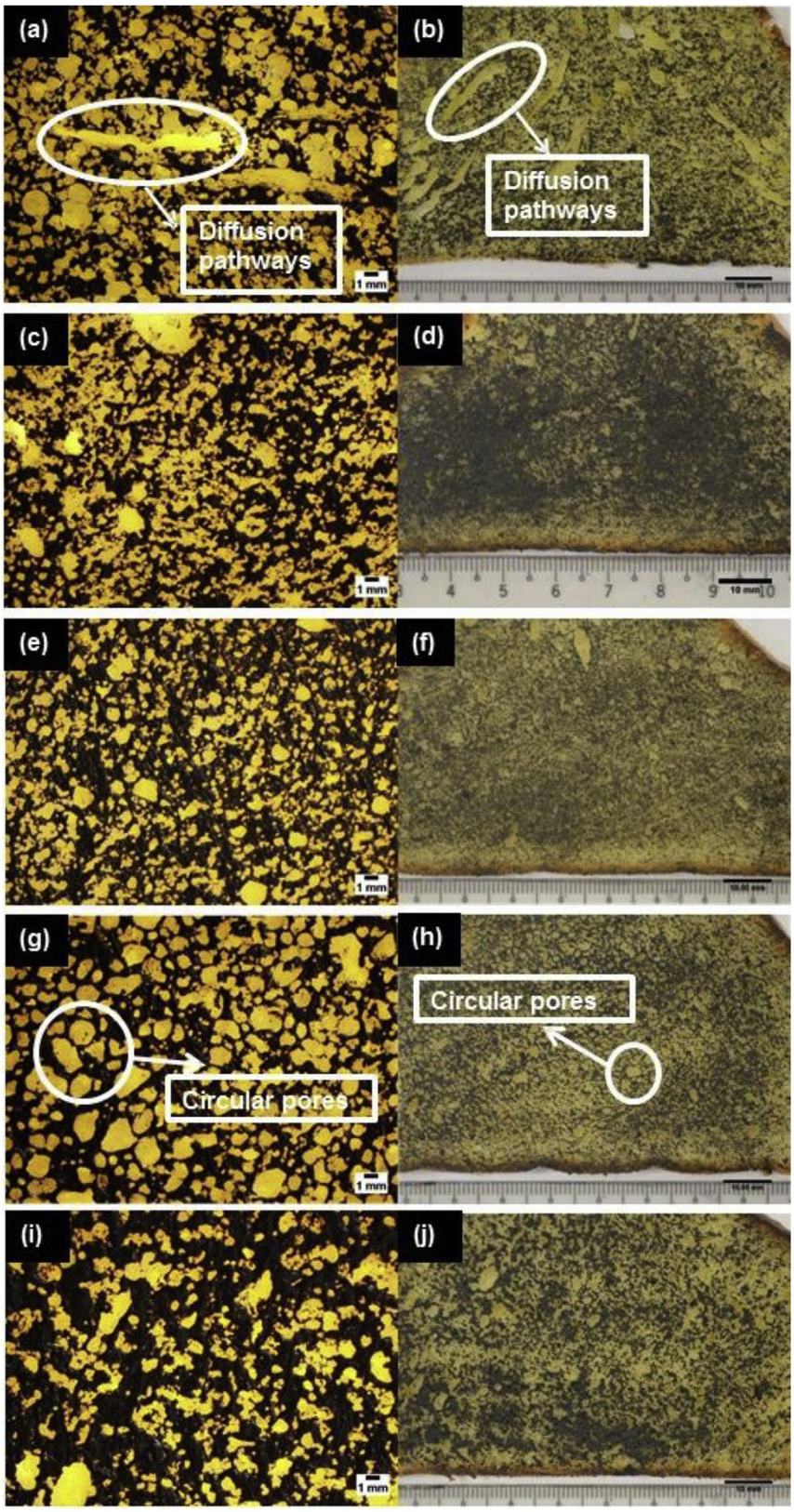

Fig. 1. Crumb structure of egg substitutes using PPI and baking additives. (a) Image of a crumb of the control under the optical microscope. (b) Image of a crumb of the control under the camera. (c) Image of a crumb of a PPI-substituted cake under the optical microscope. (d) Image of a crumb of a PPI-substituted cake under the camera. (e) Image of a PPI + XN-substituted cake under the optical microscope. (f) Image of a PPI + XN-substituted cake under the camera. (g) Image of a PPI + XN + MDG-substituted cake under the optical microscope. (h) Image of a PPI + XN + MDG-substituted cake under the camera. (i) Image of a PPI + XN + S-substituted cake under the optical microscope. (j) Image of a PPI + XN + SL-substituted cake under the camera. PPI – isolated pea protein; XN – xanthan gum; MDG – mono, diglycerides; SL – soy lecithin. Fig. 1(a) and (b)–Reprinted from Lin et al. (2017). Copyright with permission from Elsevier.

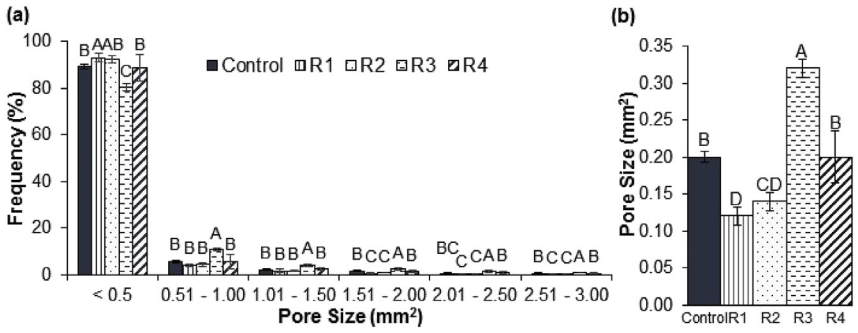

Fig. 2. Effect of egg replacement on the crumb structure. (a) Pore area distribution of cakes using PPI and other baking additives as egg substitutes. (b) Average pore size of pea protein based eggless cakes under different treatments. Mean values with different letters are significantly different ($P < 0.05$). R1: PPI; R2: PPI + 0.1% XN; R3: PPI + 0.1% XN + 1% MDG; R4: PPI + 0.1% XN + 1% SL. PPI - isolated pea protein; XN – xanthan gum; MDG – mono, diglycerides; SL – soy lecithin.

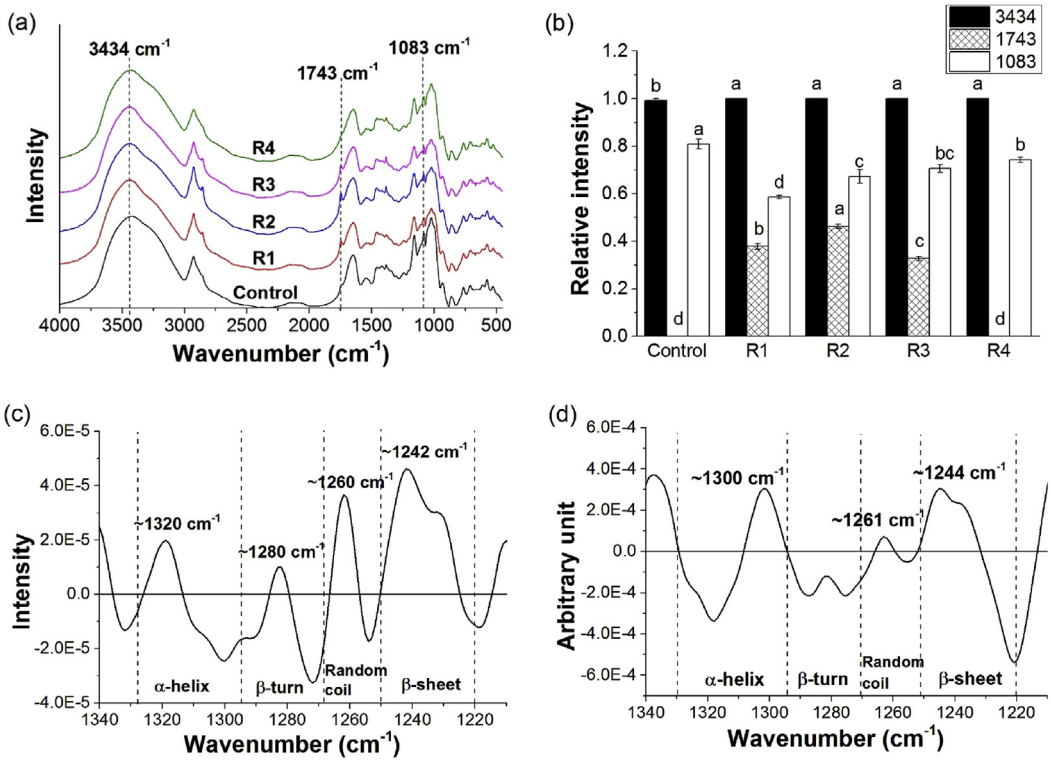

Fig. 3. (a) Fourier transform infrared spectroscopy (FTIR) spectra of starch in cakes from different recipes; (b) Relative intensities of peaks at 3434, 1743, and 1083 cm^{-1}; Inverted second derivative spectrum of (c) gliadin and (d) glutenin in amide III region (1350–1200 cm^{-1}). R1: PPI; R2: PPI + 0.1% XN; R3: PPI + 0.1% XN + 1% MDG; R4: PPI + 0.1% XN + 1% SL. PPI – isolated pea protein; XN – xanthan gum; MDG – mono, diglycerides; SL – soy lecithin.

structure of glutens. The traditional approach of deconvolution on the amide I region was unsuccessful here because of variation and inconsistency with respect to the assignment of the fitted peaks to α-helix, random coils, and β-turn (Bock & Damodaran, 2013; Byler & Susi, 1986). Thereby, amide III was used for the secondary structure analysis for gliadins to obtain better separations and more accurate results.

Amide III was divided into four sections, as displayed in Fig. 3c, and it was obvious that the four components showed little overlap. The results in Table 3 indicated that the major secondary structure of all the groups were β-sheets, which was consistent with the previous studies of Wang et al. (2015). The band centred at 1300–1304 cm^{-1} was assigned to the α-helix, resulting in no β-turn in the protein. The β-turn structure was dominant in the repetitive domain of glutenin (Shewry, Popineau, Lafiandra, & Belton, 2000) and some studies assigned a typical α-helix band to the combination of unordered structure, β-turn, and glutamine residues (Feeney et al., 2003). Alpha-helices and β-turns are both helical structures, only differing in the number of molecules in a helix (four for a β-turn and five for an α-helix). As a result, the peak at around 1300 cm^{-1} might represent a mixture of the two helical conformations, or some intermediate structures between these two forms.

Compared with the sample with only PPI as the substitute, the β-sheets in gliadin were observed to be converted to unordered structures and β-turns upon the combinations with other ingredients. XN (0.1%) notably enhanced the conversion of both components. When PPI, XN, and any of the emulsifiers were mixed, combination effects were observed: SL could add to the effects, while MDG seemed maintain the level. Thus, a similar content of β-

sheets was turned into random coil and β-turns in R3 group, whereas even more was converted in R4. In contrast to the control group, the total contents of β-turns and α-helix increased with the addition of various PPI substitutes. This reflected the improvements in hydrogen bond strength in the gliadins in these eggless recipes.

The "loop and train" model postulated that their major parts, especially high molecular weight glutenin subunits, contained repetitive domains, which adopted β-turns and intermolecular β-sheets to build up the loop and train structures (Shewry et al., 2000). As a result, the content of intermolecular β-sheets should be quantified in addition to the total contents, thus the bands at about 1611 and 1625 cm^{-1} in the amide I region were also analysed. As presented in Table 3, the β-sheet content was slightly decreased upon addition of food additives in the eggless cakes (R2-4). XN tended to convert β-sheets into the random coils, while the existence of any emulsifier converted β-sheets into helical structures. PPI seemed to strengthen the interactions in the repetitive regions, resulting in increased intermolecular β-sheets and fewer helical structures. When XN was added with PPI, no significant alteration was detected for the intermolecular β-sheets; thus it was the other β-sheet structure that became unordered. Incorporating the emulsifiers appeared to increase the ordering of the glutenin structures; however, the intermolecular β-sheets also decreased. Thus, more β-sheet structures, as well as α-helices/β-turns were formed. A possible explanation was that the resulting emulsifying effect loosened the repetitive domains and remarkably decreased the intermolecular hydrogen bonds. This might also account for the much lower content of intermolecular β-sheets in the control group.

3.6. AFM analysis of glutens

In addition to the secondary structures, the morphologies of the glutens were also imaged by AFM (Liu & Wang, 2011). In the AFM images (Fig. 4a), the overall profiles are continuous sheets embedded with many spherical aggregates of various sizes. A previous study of glutens' architectural changes in response to different conditions focused more on the whole gluten (Wang et al., 2015) or on the fractions of gliadin (McMaster, Miles, Kasarda, Shewry, & Tatham, 2000). However, it is probably the bulk morphology resulting from the interactions between these fractions that is more crucial to the final quality of the batter and cakes. Therefore, this analysis was more dependent on the comparisons among our own results.

The gliadin aggregates were categorised into four groups based on their sizes (Fig. 4b). For the conventional cakes, the aggregates were relatively small (100–200 nm), indicative of a small and homogeneous aggregate profile. When PPI was incorporated into the cakes, the aggregate tended to become larger and were distributed over a wider range. The combination of PPI, XN, and either of the emulsifiers showed comparable effects on aggregation, both shifting to medium sizes (200–300 nm). It could be assumed that the smaller particles were bound with the adjacent ones to form larger particles. The additives, both hydrocolloid and emulsifiers, then interfered with the conformations mainly through hydrogen bonding and hydrophobic interaction. In brief, when the substitutes were used to replace eggs, the gliadin aggregates appeared to be larger and less homogeneous because of the integration of PPI molecules. There may be potential relationships between the sum of β-turn and α-helix structure contents and the gliadin aggregate size. The lowest content of helical structures in the control group might be related to the finding that the aggregates were mostly in the smaller size range, according to the microscopy results.

AFM also gave a more visualised understanding of the conformations of glutenins. The sheet-like structures ranged from 5 to 11 nm in thickness and there were no significant differences between the control (6.85 nm) and the treated groups of R1 (7.77 nm) and R4 (6.17 nm) (Table 4 & Fig. 5e). The thin layers were assumed to be formed by piled high molecular weight glutenin polymers (Shewry et al., 2000). In terms of the networking structures, most of the glutenin samples showed some kind of pores, except the R1 eggless cake (Fig. 5). According to their size and morphology, the porous regions were presumed to be the hydrophilic positions where hydrated water molecules were bound (Jiang, Kontogiorgos, Kasapis, & Douglas Goff, 2008).

Fig. 5a indicated that the pores of the control group were larger and that some might be merged with others to yield open-cell pores. When PPI was added, the overall areas of porosity decreased obviously. In the cake with PPI only as the substitute, the glutenin appeared to be too compacted to produce any pores. Upon the inclusion of other additives, the came became more porous. With the help of XN, closed-cell pores were created (Fig. 5b), which became smaller when MDG or SL was also added (Fig. 5c and d). The open-cell pores in the control cakes were probably caused by the presence of lecithin in the yolk, which might have contributed remarkably to the hydrophilic interactions between glutenin and water molecules, leading to a large area of porosity. In contrast, PPI tended to form a thin viscoelastic film enclosing the foams to protect them from rupture (Sahi & Alava, 2003), leading to closed-cell structures in the eggless cakes.

4. Conclusions

Egg substitutes containing PPI + 0.1% XN + 1% SL (R4) resulted in eggless cakes with similar batter specific gravity (1.01 *vs.* 1.03), crumb colour (a* at 0.09 *vs.* −0.04), crumb pore properties (average pore area both at about 0.20 mm^2) with respect to the physical properties to those of the traditional cake. Although the effects of

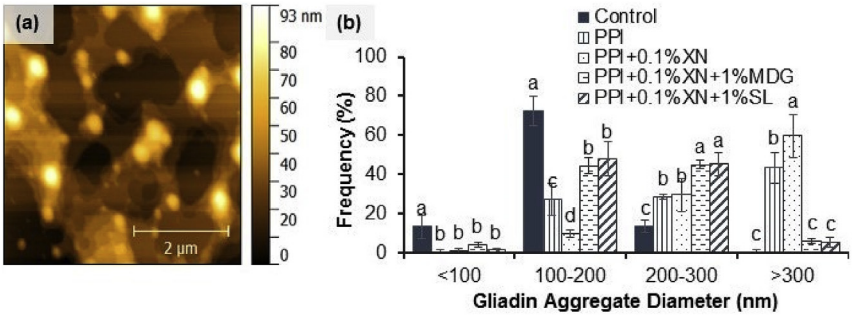

Fig. 4. (a) Atomic force microscopy (AFM) images of gliadin structures; (b) Size distribution of gliadin aggregates in eggless cake with PPI substitutes. Within each size range, groups with different letters are significantly different ($P < 0.05$). PPI - isolated pea protein; XN – xanthan gum; MDG – mono, diglycerides; SL – soy lecithin.

Table 4
Nanostructure of glutenin in eggless cakes with PPI substitutes.

Group	Layer height (nm)	Pore number per 25 μm^2	Pore size distribution (nm)^			
			<100	100–500	500–1000	>1000
Control	6.85 ± 0.77^{BC}	5 ± 1^{C}	0%	5%	16%	79%
R1	7.77 ± 1.15^{B}	–	–	–	–	–
R2	10.56 ± 2.70^{A}	24 ± 3^{B}	0%	59%	23%	18%
R3	5.53 ± 1.02^{D}	64 ± 9^{A}	40%	60%	0%	0%
R4	6.17 ± 1.03^{CD}	66 ± 4^{A}	18%	82%	0%	0%

^ The pore size distribution was calculated based on 90 pores for the control group and at least 100 pores for the other groups.
*R1: PPI; R2: PPI + 0.1% XN; R3: PPI + 0.1% XN + 1% MDG; R4: PPI + 0.1% XN + 1% SL. PPI – isolated pea protein; XN – xanthan gum; MDG – mono, diglycerides and SL – soy lecithin. Mean values with different letters indicate significantly differences ($P < 0.05$).

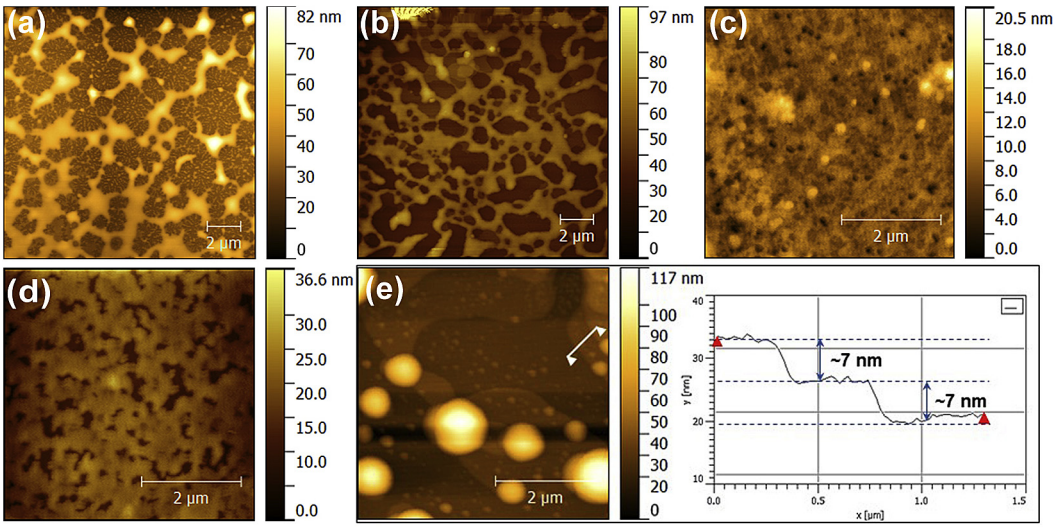

Fig. 5. Atomic force microscopy (AFM) images of glutenin protein in eggless cake with PPI substitutes. Porous structure of (a) traditional cake and eggless cakes with (b) PPI + 0.1% XN, (c) PPI + 0.1% XN + 1% MDG and (d) PPI + 0.1% XN + 1% SL; (e) Example of thin layer structure. PPI - isolated pea protein; XN – xanthan gum; MDG – mono, diglycerides; SL – soy lecithin.

the substitutes on the structural properties of starches and glutens were not sufficiently clear, some similarities between the R4 and control cakes were observed, including the intensity ratio of 1047/1022 (both 0.55) in FTIR spectra of starch and the secondary structures of glutenin (20.13% *vs.* 20.45% for intermolecular β-sheets). However, cakes baked using formulation R4 were unable to match the specific volume (1.87 *vs.* 2.17 cm^3/g) and the gliadin conformational attributes of the control cakes. Nonetheless, these promising results indicated that eggs could be replaced in cakes, albeit not easily.

Acknowledgements

This work was supported by an industry grant from Guangzhou Welbon Biological Technology Co., Ltd. (R-143-000-577-597).

References

An, H., Liang, H., Liu, Z., Yang, H., Liu, Q., & Wang, H. (2011). Nano-structures of debranched potato starch obtained by isoamylolysis. *Journal of Food Science, 76*(1), N11–N14.
Ashwini, A., Jyotsna, R., & Indrani, D. (2009). Effect of hydrocolloids and emulsifiers on the rheological, microstructural and quality characteristics of eggless cake. *Food Hydrocolloids, 23*(3), 700–707.
Baixauli, R., Sanz, T., Salvador, A., & Fiszman, S. M. (2008). Muffins with resistant starch: Baking performance in relation to the rheological properties of the batter. *Journal of Cereal Science, 47*(3), 502–509.
Bock, J. E., & Damodaran, S. (2013). Bran-induced changes in water structure and gluten conformation in model gluten dough studied by Fourier transform infrared spectroscopy. *Food Hydrocolloids, 31*(2), 146–155.
Byler, D. M., & Susi, H. (1986). Examination of the secondary structure of proteins by deconvolved FTIR spectra. *Biopolymers, 25*(3), 469–487.
Chong, J. X., Lai, S., & Yang, H. (2015). Chitosan combined with calcium chloride impacts fresh-cut honeydew melon by stabilising nanostructures of sodium-carbonate-soluble pectin. *Food Control, 53*, 195–205.
Du, X., An, H., Liu, Z., Yang, H., & Wei, L. (2014). Probing starch–iodine interaction by atomic force microscopy. *Scanning, 36*(4), 394–400.
Feeney, K. A., Wellner, N., Gilbert, S. M., Halford, N. G., Tatham, A. S., Shewry, P. R., et al. (2003). Molecular structures and interactions of repetitive peptides based on wheat glutenin subunits depend on chain length. *Biopolymers, 72*(2), 123–131.
Feng, X., Bansal, N., & Yang, H. (2016). Fish gelatin combined with chitosan coating inhibits myofibril degradation of golden pomfret (*Trachinotus blochii*) fillet during cold storage. *Food Chemistry, 200*, 283–292.
Feng, X., Fu, C., & Yang, H. (2017). Gelatin addition improves nutrient retention, texture and mass transfer of fish balls without altering their nanostructure during boiling. *LWT-Food Science and Technology, 77*, 142–151.
Feng, X., Ng, V. K., Mikš-Krajnik, M., & Yang, H. (2017). Effects of fish gelatin and tea polyphenol coating on the spoilage and degradation of myofibril in fish fillet during cold storage. *Food and Bioprocess Technology, 10*(1), 89–102.
Gómez, M., Ronda, F., Caballero, P. A., Blanco, C. A., & Rosell, C. M. (2007). Functionality of different hydrocolloids on the quality and shelf-life of yellow layer cakes. *Food Hydrocolloids, 21*(2), 167–173.
Hesso, N., Le-Bail, A., Loisel, C., Chevallier, S., Pontoire, B., Queveau, D., et al. (2015). Monitoring the crystallization of starch and lipid components of the cake crumb during staling. *Carbohydrate Polymers, 133*, 533–538.
Hicsasmaz, Z., Yazgan, Y., Bozoglu, F., & Katnas, Z. (2003). Effect of polydextrose-substitution on the cell structure of the high-ratio cake system. *LWT - Food Science and Technology, 36*(4), 441–450.
Hoang, H. D. (2012). *Evaluation of pea protein and modified pea protein as egg replacers*. Unpublished doctoral dissertation. North Dakota State University.
Horwitz, W. (1980). *Official methods of analysis* (Vol. 534). AOAC Arlington, VA: Washington DC.
Jiang, B., Kontogiorgos, V., Kasapis, S., & Douglas Goff, H. (2008). Rheological investigation and molecular architecture of highly hydrated gluten networks at subzero temperatures. *Journal of Food Engineering, 89*(1), 42–48.

Ji, N., Li, X., Qiu, C., Li, G., Sun, Q., & Xiong, L. (2015). Effects of heat moisture treatment on the physicochemical properties of starch nanoparticles. *Carbohydrate Polymers, 117*, 605–609.
Kiosseoglou, V., & Paraskevopoulou, A. (2014). Eggs. In W. Zhou, Y. H. Hui, I. D. Leyn, M. A. Pagani, C. M. Rosell, J. D. Selman, et al. (Eds.), *Bakery products science and Technology* (pp. 243–258). Chichester: John Wiley & Sons, Ltd.
Lakshminarayan, S. M., Rathinam, V., & KrishnaRau, L. (2006). Effect of maltodextrin and emulsifiers on the viscosity of cake batter and on the quality of cakes. *Journal of the Science of Food and Agriculture, 86*(5), 706–712.
Lin, M., Tay, S. H., Yang, H., Yang, B., & Li, H. (2017). Replacement of eggs with soybean protein isolates and polysaccharides to prepare yellow cakes suitable for vegetarians. *Food Chemistry, 229*, 663–673.
Liu, H., Chen, F., Lai, S., Tao, J., Yang, H., & Jiao, Z. (2017). Effects of calcium treatment and low temperature storage on cell wall polysaccharide nanostructures and quality of postharvest apricot (Prunus armeniaca). *Food Chemistry, 225*, 87–97.
Liu, H., Liang, R., Antoniou, J., Liu, F., Shoemaker, C. F., Li, Y., et al. (2014). The effect of high moisture heat-acid treatment on the structure and digestion property of normal maize starch. *Food Chemistry, 159*, 222–229.
Liu, Q., Tan, C. S. C., Yang, H., & Wang, S. (2017). Treatment with low-concentration acidic electrolysed water combined with mild heat to sanitise fresh organic broccoli (*Brassica oleracea*). *LWT-Food Science and Technology, 79*, 594–600.
Liu, S., & Wang, Y. (2011). A review of the application of atomic force microscopy(AFM) in food science and technology. *Advances in Food and Nutrition Research, 62*, 201–240.
Lookhart, G., & Bean, S. (1995). Separation and characterization of wheat protein fractions by high-performance capillary electrophoresis. *Cereal Chemistry, 72*(6), 527–532.
Luo, Q., Lui, M., Xu, Y., Ionescu, M., & Petrovic, Z. S. (2013). Thermosetting allyl resins derived from soybean fatty acids. *Journal of Applied Polymer Science, 127*(1), 432–438.
Mao, L., & Miao, S. (2015). Structuring food emulsions to improve nutrient delivery during digestion. *Food Engineering Reviews, 7*(4), 439–451.
Mao, J., Zhang, L., Chen, F., Lai, S., Yang, B., & Yang, H. (2017). Effect of vacuum impregnation combined with calcium lactate on the firmness and polysaccharide morphology of Kyoho grapes (Vitis vinifera x V. labrusca). *Food and Bioprocess Technology, 10*(4), 699–709.
McMaster, T. J., Miles, M. J., Kasarda, D. D., Shewry, P. R., & Tatham, A. S. (2000). Atomic force microscopy of a-gliadin fibrils and in situ degradation. *Journal of Cereal Science, 31*(3), 281–286.
Miao, M., Jiang, B., Zhang, T., Jin, Z., & Mu, W. (2011). Impact of mild acid hydrolysis on structure and digestion properties of waxy maize starch. *Food Chemistry, 126*(2), 506–513.
Primo-Martín, C., van Nieuwenhuijzen, N. H., Hamer, R. J., & van Vliet, T. (2007). Crystallinity changes in wheat starch during the bread-making process: Starch crystallinity in the bread crust. *Journal of Cereal Science, 45*(2), 219–226.
Rahmati, N. F., & Mazaheri Tehrani, M. (2014). Replacement of egg in cake: Effect of soy milk on quality and sensory characteristics. *Journal of Food Processing and Preservation, 39*(6), 574–582.
Ratnayake, W. S., Geera, B., & Rybak, D. A. (2012). Effects of egg and egg replacers on yellow cake product quality. *Journal of Food Processing and Preservation, 36*(1), 21–29.
Sahi, S. S., & Alava, J. M. (2003). Functionality of emulsifiers in sponge cake production. *Journal of the Science of Food and Agriculture, 83*(14), 1419–1429.
Shewry, P. R., Popineau, Y., Lafiandra, D., & Belton, P. (2000). Wheat glutenin subunits and dough elasticity: Findings of the EUROWHEAT project. *Trends in Food Science & Technology, 11*(12), 433–441.
Sow, L. C., & Yang, H. (2015). Effects of salt and sugar addition on the physicochemical properties and nanostructure of fish gelatin. *Food Hydrocolloids, 45*, 72–82.
Turabi, E., Sumnu, G., & Sahin, S. (2008). Rheological properties and quality of rice cakes formulated with different gums and an emulsifier blend. *Food Hydrocolloids, 22*(2), 305–312.
Turabi, E., Sumnu, G., & Sahin, S. (2010). Quantitative analysis of macro and microstructure of gluten-free rice cakes containing different types of gums baked in different ovens. *Food Hydrocolloids, 24*(8), 755–762.
Wang, Q., Li, Y., Sun, F., Li, X., Wang, P., Sun, J., et al. (2015). Tannins improve dough mixing properties through affecting physicochemical and structural properties of wheat gluten proteins. *Food Research International, 69*, 64–71.
Wang, Y., Su, C. P., Schulmerich, M., & Padua, G. W. (2013). Characterization of core-shell structures formed by zein. *Food Hydrocolloids, 30*(2), 487–494.
Wang, P., Xu, L., Nikoo, M., Ocen, D., Wu, F., Yang, N., et al. (2014). Effect of frozen storage on the conformational, thermal and microscopic properties of gluten: Comparative studies on gluten-, glutenin- and gliadin-rich fractions. *Food Hydrocolloids, 35*, 238–246.
Wilderjans, E., Pareyt, B., Goesaert, H., Brijs, K., & Delcour, J. A. (2008). The role of gluten in a pound cake system: A model approach based on gluten–starch blends. *Food Chemistry, 110*(4), 909–915.
Xie, X., Cui, S. W., Li, W., & Tsao, R. (2008). Isolation and characterization of wheat bran starch. *Food Research International, 41*(9), 882–887.
Yang, H. (2014). *Atomic force microscopy (AFM): Principles, modes of operation and limitations*. Hauppauge, New York: Nova Science Publishers, Inc.
Yang, H., Wu, Q., Ng, L. Y., & Wang, S. (2017). Effects of vacuum impregnation with calcium lactate and pectin methylesterase on quality attributes and chelate-soluble pectin morphology of fresh-cut papayas. *Food and Bioprocess Technology*. http://dx.doi.org/10.1007/s11947-017-1874-7.
Zhang, L., Chen, F., Zhang, P., Lai, S., & Yang, H. (2017). Influence of rice bran wax coating on the physicochemical properties and pectin nanostructure of cherry tomatoes. *Food and Bioprocess Technology, 10*(2), 349–357.
Zhang, S., Lu, Q., Yang, H., & Meng, D. (2011). Effects of protein content, glutenin-to-gliadin ratio, amylose content and starch damage on textural properties of Chinese fresh white noodles. *Cereal Chemistry, 88*(3), 296–301.